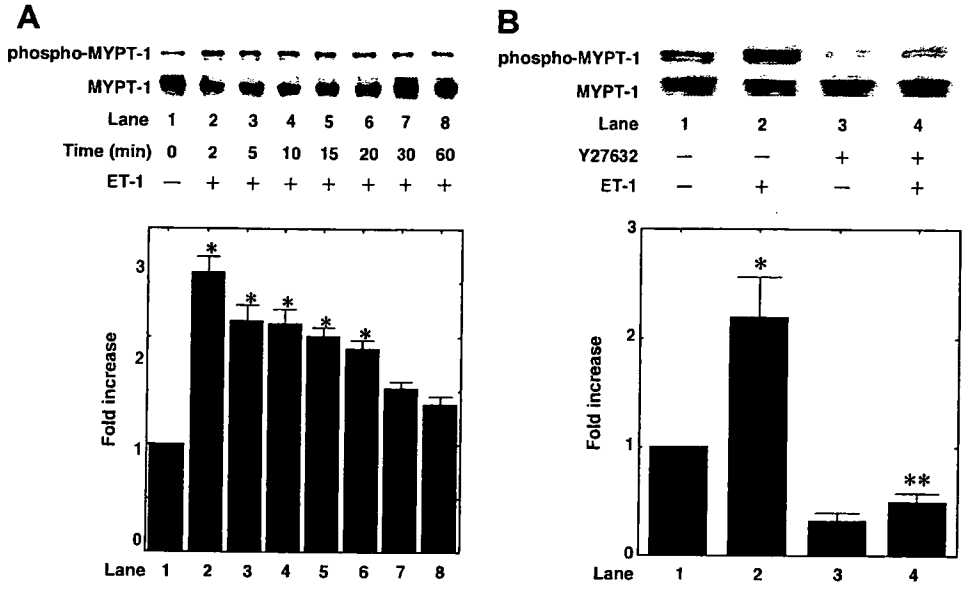

Fig. 1. Effect of ET-1 on the phosphorylation of MYPT-1 and effect of Y27632 on the ET-1-induced phosphorylation of MYPT-1 in MC3T3-E1 cells. (A) The cultured cells were stimulated by 0.1 μM ET-1 for the indicated periods. (B) The cultured cells were pretreated with 10 μM Y27632 or vehicle for 60 min, and then stimulated by 0.1 μM ET-1 or vehicle for 2 min. The extracts of cells were subjected to SDS–PAGE with subsequent Western blotting analysis with antibodies against phospho-specific MYPT-1 or MYPT-1. The histogram shows quantitative representations of the levels of ET-1-induced phosphorylation obtained from laser densitometric analysis of three independent experiments. Each value represents the mean ± SEM of triplicate determinations. Similar results were obtained with two additional and different cell preparations. $^{*}p < 0.05$, compared to the value of control. $^{**}p < 0.05$, compared to the value of ET-1 alone.

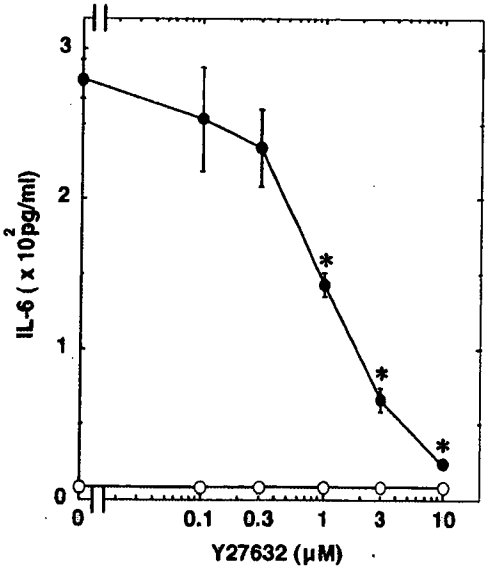

Fig. 2. Effect of Y27632 on the ET-1-induced IL-6 synthesis in MC3T3-E1 cells. The cultured cells were pretreated with various doses of Y27632 for 60 min, and then stimulated by 0.1 μM ET-1 or vehicle for 48 h. Each value represents the mean ± SEM of triplicate determinations. Similar results were obtained with two additional and different cell preparations. $^{*}p < 0.05$, compared to the value of ET-1 alone.

transduce the various messages of a variety of agonists [25]. In our previous studies [13,14], we have shown that ET-1 stimulates IL-6 synthesis via p44/p42 MAP kinase and p38 MAP kinase but not SAPK/JNK among the MAP kinase superfamily in osteoblast-like MC3T3-E1 cells. In order to investigate whether Rho-kinase-effect on the ET-1-stimulated IL-6 synthesis is dependent upon the activation of p44/p42 MAP kinase or p38 MAP kinase in MC3T3-E1 cells, we next examined the effect of Y27632 on the phosphorylation of p44/p42 MAP kinase by ET-1. However, Y27632 failed to affect the ET-1-induced phosphorylation of p44/p42 MAP kinase (Fig. 3).

Table 1
Effect of fasudil on the ET-1-stimulated IL-6 synthesis in MC3T3-E1 cells

Fasudil (μM)	ET-1	IL-6 (pg/ml)
0	−	<7.8
0	+	287 ± 16*
0.3	−	<7.8
0.3	+	261 ± 6
1	−	<7.8
1	+	171 ± 5**
3	−	<7.8
3	+	70 ± 5**

The cultured cells were pretreated with various doses of fasudil for 60 min, and then stimulated by 0.1 μM ET-1 or vehicle for 48 h. Each value represents the mean ± SEM of triplicate determinations. Similar results were obtained with two additional and different cell preparations.
* $p < 0.05$, compared to the control.
** $p < 0.05$, compared to the value of ET-1 alone.

Effects of Y27632 or fasudil on the ET-1-induced phosphorylation of p38 MAP kinase in MC3T3-E1 cells

In addition, we examined effect of Y27632 on the ET-1-induced phosphorylation of p38 MAP kinase in MC3T3-E1 cells. Y27632, which itself had little effect on

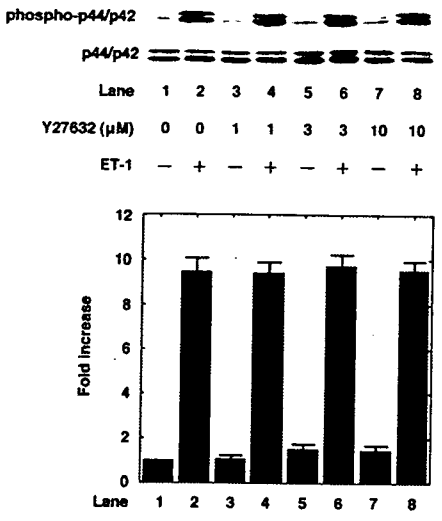

Fig. 3. Effect of Y27632 on the ET-1-induced phosphorylation of p44/p42 MAP kinase in MC3T3-E1 cells. The cultured cells were pretreated with various doses of Y27632 for 60 min, and then stimulated by 0.1 μM ET-1 or vehicle for 5 min. The extracts of cells were subjected to SDS–PAGE with subsequent Western blotting analysis with antibodies against phospho-specific p44/p42 MAP kinase or p44/p42 MAP kinase. The histogram shows quantitative representations of the levels of ET-1-induced phosphorylation obtained from laser densitometric analysis of three independent experiments. Each value represents the mean ± SEM of triplicate determinations. Similar results were obtained with two additional and different cell preparations.

the phosphorylation of p38 MAP kinase, markedly suppressed the ET-1-induced phosphorylation of p38 MAP kinase (Fig. 4A). The Y27632-effect on the phosphorylation levels was dose-dependent in the range between 1 and 10 μM. Y27632 (10 μM) caused about 80% inhibition in the ET-1-effect.

Fasudil attenuated the ET-1-induced levels of phosphorylated-p38 MAP kinase (Fig. 4B). The inhibitory effect of fasudil was dose-dependent in the range between 1 and 10 μM. Fasudil (10 μM) caused approximately 70% inhibition in the ET-1-effect.

Discussion

In the present study, we found that ET-1 time-dependently induced the phosphorylation of MYPT-1 in osteoblast-like MC3T3-E1 cells, using phospho-specific MYPT-1 (Thr850) antibodies. It is generally recognized that MYPT is a myosin-binding subunit of myosin phosphatase, which regulates the interaction of actin and myosin, and a downstream target of Rho-kinase [15,24]. In addition, we found that Rho-kinase inhibitors [16] such as Y27632 and fasudil truly reduced the ET-1-induced phosphorylation levels of MYPT-1. Taking our findings into account, it is most likely that ET-1 stimulates the activation of Rho-kinase in osteoblast-like MC3T3-E1 cells.

We next investigated whether Rho-kinase functions in the ET-1-stimulated IL-6 synthesis or not in osteoblast-like MC3T3-E1 cells. The ET-1-stimulated synthesis of IL-6 was significantly suppressed by Y27632, a specific inhibitor of Rho-kinase [16]. We confirmed that the Rho-kinase inhibitor truly reduced the ET-1-induced phosphorylation levels of MYPT-1. It seems that the activated Rho-kinase acts as a positive regulator in the IL-6 synthesis by ET-1 in osteoblast-like MC3T3-E1 cells. In addition, the ET-1-

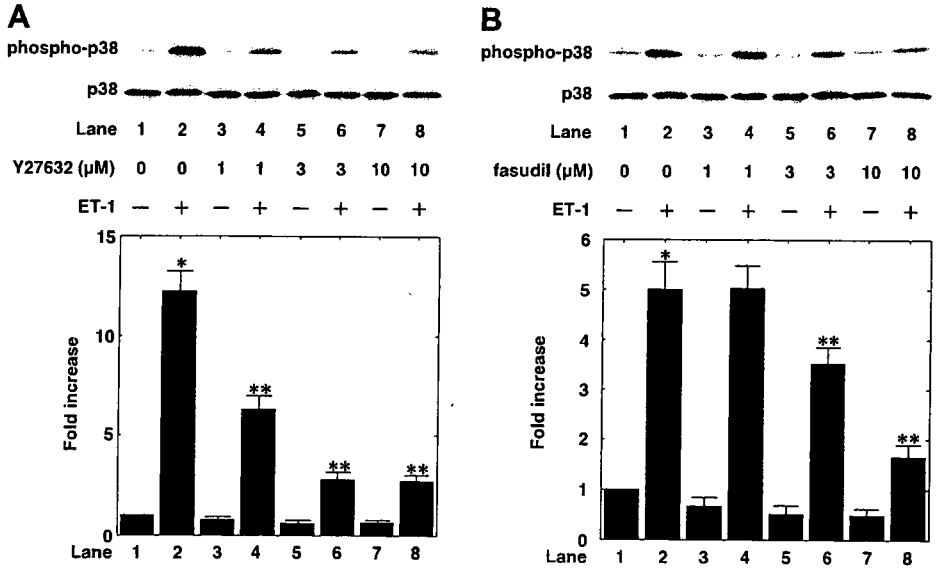

Fig. 4. Effects of Y27632 or fasudil on the ET-1-induced phosphorylation of p38 MAP kinase in MC3T3-E1 cells. The cultured cells were pretreated with various doses of Y27632 (A) or fasudil (B) for 60 min, and then stimulated by 0.1 μM ET-1 or vehicle for 20 min. The extracts of cells were subjected to SDS–PAGE with subsequent Western blotting analysis with antibodies against phospho-specific p38 MAP kinase or p38 MAP kinase. The histogram shows quantitative representations of the levels of ET-1-induced phosphorylation obtained from laser densitometric analysis of three independent experiments. Each value represents the mean ± SEM of triplicate determinations. Similar results were obtained with two additional and different cell preparations. $^{*}p < 0.05$, compared to the control. $^{**}p < 0.05$, compared to the value of ET-1 alone.

stimulated IL-6 synthesis as well as the phosphorylated levels of MYPT-1 was inhibited by fasudil, another Rho-kinase inhibitor [16]. Therefore, based on our results, it is most likely that ET-1 activates Rho-kinase, resulting in up-regulation of IL-6 synthesis in osteoblast-like MC3T3-E1 cells.

Regarding about IL-6 synthesis, we have previously demonstrated that the ET-1 stimulated IL-6 synthesis is mediated by activation of p44/p42 MAP kinase and p38 MAP kinase but not SAPK/JNK among the MAP kinase superfamily in osteoblast-like MC3T3-E1 cells [13,14]. Additionally, we investigated the relationship between Rho-kinase and these MAP kinases in the IL-6 synthesis in MC3T3-E1 cells. However, Y27632 failed to affect the ET-1-induced phosphorylation levels of p44/p42 MAP kinase. Therefore, it seems unlikely that Rho-kinase affects the ET-1-stimulated IL-6 synthesis through the modulation of p44/p42 MAP kinase in osteoblast-like MC3T3-E1 cells. On the contrary, the ET-1-induced phosphorylation levels of p38 MAP kinase were significantly suppressed by Y27632 and fasudil. These results suggest that Rho-kinase regulates the ET-1-stimulated IL-6 synthesis via p38 MAP kinase. In the present study, the maximum effect on the phosphorylation of MYPT-1, a well-known downstream target of Rho-kinase [15], was observed within 2 min after the ET-1 stimulation. In our previous study [26], we have shown that the phosphorylation of p38 MAP kinase reach the peak at 20 min after the stimulation of ET-1 in MC3T3-E1 cells. The time course of the phosphorylation of MYPT-1 stimulated by ET-1 seems to be faster than that of p38 MAP kinase, in turn, ET-1-induced activation of p38 MAP kinase subsequently occurs after the Rho-kinase activation. Taking our findings into account as a whole, it is most likely that Rho-kinase acts at a point upstream from p38 MAP kinase in the ET-1-induced IL-6 synthesis in osteoblast-like MC3T3-E1 cells.

Rho-kinase is currently recognized to play a pivotal role in various cellular functions, especially vascular smooth muscle contraction [15,16]. In bone metabolism, it has been reported that the Rho-kinase pathway acts as a negative regulator of osteoblast differentiation and induces osteoblast proliferation [19]. Our present results indicate that Rho-kinase activation in osteoblasts has an important role in the control of the production of IL-6, one of the key regulators of bone metabolism. It is well known that IL-6 produced by osteoblasts is a potent bone resorptive agent and induces osteoclast formation [3,5]. In addition, it is recognized that ET-1 acts as a bone resorptive agent in bone metabolism [10]. Evidence is recently accumulating that tumor cells produces ET-1 which mediates bone metastasis by stimulating the proliferation of osteoblasts and new bone formation [11]. Therefore, our present findings lead us to speculate that ET-1-activated Rho-kinase acts as a positive regulator of bone resorption via the fine tuning of local cytokine network. Therefore, the Rho-kinase pathway in osteoblasts might be considered to be a new candidate as a molecular therapeutic target of bone resorption and osteoblastic bone metastases due to breast or prostate cancer. The pathophysiological significance of regulatory mechanism by Rho-kinase in osteoblasts remains still unclear. Further investigation is necessary to clarify the exact role of Rho-kinase in osteoblasts.

In conclusion, our results strongly suggest that Rho-kinase regulates the ET-1-stimulated IL-6 synthesis at a point upstream from p38 MAP kinase in osteoblasts.

Acknowledgments

We are very grateful to Yoko Kawamura and Seiko Sakakibara for their skillful technical assistance. This investigation was supported in part by Grant-in-Aid for Scientific Research (16590873 and 16591482) for the Ministry of Education, Science, Sports and Culture of Japan, the Research Grants for Longevity Sciences (15A-1 and 15C-2), Research Grant on Proteomics and Research Grant on Longevity Sciences from the Ministry of Health, Labour and Welfare of Japan.

References

[1] S. Akira, T. Taga, T. Kishimoto, Interleukin-6 in biology and medicine, Adv. Immunol. 54 (1993) 1–78.
[2] D. Heymann, A.V. Rousselle, gp130 Cytokine family and bone cells, Cytokine 12 (2000) 1455–1468.
[3] S. Kwan Tat, M. Padrines, S. Theoleyre, D. Heymann, Y. Fortun, IL-6 is produced by osteoblasts and induces bone resorption, Cytokine Growth Factor Rev. 15 (2004) 49–60.
[4] P.J. Nijweide, E.H. Burger, J.H.M. Feyen, Cells of bone: proliferation, differentiation, and hormonal regulation, Physiol. Rev. 86 (1986) 855–886.
[5] Y. Ishimi, C. Miyaura, C.H. Jin, T. Akatsu, F. Abe, Y. Nakamura, Y. Yamaguchi, S. Yoshiki, T. Matsuda, T. Hirano, T. Kishimoto, T. Suda, IL-6 is produced by osteoblasts and induces bone resorption, J. Immunol. 145 (1990) 3297–3303.
[6] G.D. Roodman, Interleukin-6: an osteotropic factor? J. Bone Miner. Res. 7 (1992) 475–478.
[7] M. Helle, J.P.J. Brakenhoff, E.R. DeGroot, L.A. Aarden, Interleukin 6 is involved in interleukin 1-induced activities, Eur. J. Immunol. 18 (1998) 957–959.
[8] A.J. Littlewood, J. Russil, G.R. Harvey, D.E. Hughes, R.G.G. Russel, M. Gowen, The modulation of the expression of IL-6 and its receptor in human osteoblasts in vitro, Endocrinology 129 (1991) 1513–1520.
[9] T. Miyauchi, T. Masaki, Pathophysiology of endothelin in the cardiovascular system, Annu. Rev. Physiol. 61 (1999) 391–415.
[10] P.H. Stern, A. Tatrai, D.E. Semler, S.K. Lee, P. Lakatos, P.J. Strieleman, G. Tarjan, J.L. Sanders, Endothelin receptors, second messengers, and actions in bone, J. Nutr. 125 (1995) 2028S–2032S.
[11] T.A. Guise, J.J. Yin, K.S. Mohammad, Role of endothelin-1 in osteoblastic bone metastases, Cancer 97 (2003) 779–784.
[12] A. Suzuki, J. Shinoda, Y. Watanabe-Tomita, N. Ozaki, Y. Oiso, O. Kozawa, ET_A receptor mediates the signalling of endothelin-1 in osteoblast-like cells, Bone 21 (1997) 143–146.
[13] H. Kawamura, T. Otsuka, H. Tokuda, H. Matsuno, N. Niwa, N. Matsui, T. Uematsu, O. Kozawa, Involvement of p42/p44 MAP kinase in endothelin-1-induced interleukin-6 synthesis in osteoblast-like cells, Bone 24 (1999) 315–320.
[14] H. Tokuda, S. Takai, Y. Hanai, R. Matsushima-Nishiwaki, T. Hosoi, A. Harada, T. Ohta, O. Kozawa, (−)-Epigallocatechin gallate suppresses endothelin-1-induced interleukin-6 synthesis in osteoblasts: inhibition of p44/p42 MAP kinase activation, FEBS Lett. 581 (2007) 1311–1316.

[15] Y. Fukata, M. Amano, K. Kaibuchi, Rho–Rho-kinase pathway in smooth muscle contraction and cytoskeletal reorganization of non-muscle cells, Trends Pharmacol. Sci. 22 (2001) 32–39.
[16] H. Shimokawa, M. Rashid, Development of Rho-kinase inhibitors for cardiovascular medicine, Trends Pharmacol. Sci. 28 (2007) 296–302.
[17] K. Riento, A.J. Ridley, Rocks: multifunctional kinases in cell behaviour, Nat. Rev. Mol. Cell Biol. 4 (2003) 446–456.
[18] W. Windischhofer, D. Zach, G. Fauler, G. Raspotnig, H. Kofeler, H.J. Leis, Involvement of Rho and p38 MAPK in endothelin-1-induced expression of PGHS-2 mRNA in osteoblast-like cells, J. Bone Miner. Res. 17 (2002) 1774–1784.
[19] D. Harmey, G. Stenbeck, C.D. Nobes, A.J. Lax, A.E. Grigoriadis, Regulation of osteoblast differentiation by Pasteurella multocida toxin (PMT): a role for Rho GTPase in bone formation, J. Bone Miner. Res. 19 (2004) 661–670.
[20] H. Sudo, H. Kodama, Y. Amagai, S. Yamamoto, S. Kasai, In vitro differentiation and calcification in a new clonal osteogenic cell line derived from newborn mouse calvaria, J. Cell Biol. 96 (1983) 191–198.
[21] O. Kozawa, H. Tokuda, M. Miwa, J. Kotoyori, Y. Oiso, Cross-talk regulation between cyclic AMP production and phosphoinositide hydrolysis induced by prostaglandin E_2 in osteoblast-like cells, Exp. Cell Res. 198 (1992) 130–134.
[22] U.K. Laemmli, Cleavage of structural proteins during the assembly of the head of bacteriophage T4, Nature 227 (1970) 680–685.
[23] K. Kato, H. Ito, K. Hasegawa, Y. Inaguma, O. Kozawa, T. Asano, Modulation of the stress-induced synthesis of hsp27 and alpha B-crystallin by cyclic AMP in C6 rat glioma cells, J. Neurochem. 66 (1996) 946–950.
[24] M. Ito, T. Nakano, F. Erdodi, D.J. Hartshorne, Myosin phosphatase: structure, regulation and function, Mol. Cell. Biochem. 259 (2004) 197–209.
[25] C. Widmann, S. Gibson, M.B. Jarpe, G.L. Johnson, Mitogen-activated protein kinase: conservation of a three-kinase module from yeast to human, Physiol. Rev. 79 (1999) 143–180.
[26] H. Kawamura, T. Otsuka, H. Matsuno, M. Niwa, N. Matsui, K. Kato, T. Uematsu, O. Kozawa, Endothelin-1 stimulates heat shock protein 27 induction in osteoblasts: involvement of p38 MAP kinase, Am. J. Physiol. 277 (1999) E1046–E1054.

Ann Nucl Med (2007) 21:361–365
DOI 10.1007/s12149-007-0028-9

CASE REPORT

Metastasis of the gastrointestinal tract: FDG-PET imaging

Kazumasa Hayasaka · Takashi Nihashi
Toshihiro Matsuura · Tetsuya Yagi
Kazumitsu Nakashima · Yasuji Kawabata · Kengo Ito
Takashi Katoh · Keita Sakata · Atsushi Harada

Received: 6 December 2006 / Accepted: 23 March 2007

Abstract We assess the usefulness of F-18-fluoro-deoxy-glucose (FDG) positron emission tomography (PET) in the evaluation of gastrointestinal metastases. Four cases (five lesions) in which metastases from three lung cancers and one malignant fibrous histiocytoma (MFH) of the femur were found in the gastrointestinal tract were reviewed (men/women 3:1, age 63–78 years, mean 72 years). The five lesions were duodenal, jejunal metastasis, and two stomach metastases from lung carcinoma, and rectal metastasis from MFH of the femur. FDG-PET was unable to detect small masses, but it was able to detect unforeseen lesions such as gastrointestinal metastases because FDG-PET is a whole-body scan in a single-operation examination. FDG-PET imaging provided valuable information for the diagnosis of gastrointestinal metastasis.

Keywords F18-FDG-PET · Gastrointestinal tract · Secondary neoplasms

K. Hayasaka (✉) · T. Nihashi
Department of Radiology, National Center for Geriatrics and Gerontology, 36-3 Gengo, Morioka-machi, Obu 474-8511, Japan
e-mail: ckv37824@mopera.ne.jp

T. Matsuura
Department of Gastroenterology, National Center for Geriatrics and Gerontology, Obu, Japan

T. Yagi · K. Nakashima
Department of Internal Medicine, National Center for Geriatrics and Gerontology, Obu, Japan

Y. Kawabata
Department of Surgery, National Center for Geriatrics and Gerontology, Obu, Japan

K. Ito · T. Katoh
Department of Brain Science and Molecular Imaging, National Center for Geriatrics and Gerontology, Obu, Japan

K. Sakata
Department of Pathology, National Center for Geriatrics and Gerontology, Obu, Japan

A. Harada
Department of Orthopedics, National Center for Geriatrics and Gerontology, Obu, Japan

Introduction

Gastrointestinal metastases are rarely detected early, but often are detected incidentally at autopsy [1, 2]. These metastases are relatively asymptomatic and rarely pose clinical problems but sometimes manifest themselves by serious complications such as gastrointestinal perforation and intussusception [3]. From this point of view, it is important to diagnose gastrointestinal metastasis before such serious complications arise.

The useful clinical application of F-18-fluoro-deoxy-glucose (FDG) positron emission tomography (PET) in the diagnosis of tumors has been already reported [4, 5]. Because studies have reported on FDG uptake in primary gastric cancer and primary colorectal cancer [6–8], metastatic tumors of the gastrointestinal tract are also expected to take up FDG. FDG-PET can detect gastrointestinal metastases, allowing their diagnosis before the development of serious complications.

The PET database of the National Center Hospital for Geriatric Medicine was retrospectively searched for all patients who had undergone a whole-body FDG-PET scan for tumor detection during the period of July 1996 to June 2006. A total of 308 subjects were studied for tumor detection. Of these, four cases (five lesions) in

Table 1 Clinical and fluoro-deoxyglucose positron emission tomography data

Case	Age/sex	Symptom	Metastatic site	Primary site	Pathology	Mean SUV in the early scan	Mean SUV in the delayed scan	Tumor size (cm)
1	78/M	Nausea	Duodenum Jejunum	Lung	Adenocarcinoma	8.5	9.2	3
2	76/M	Bloody stool	Rectum	Femoral bone	Adenocarcinoma	5.8	8.1	2
3	63/M	Abdominal discomfort	Stomach	Lung	MFH	5.1	ND	4.5
4	72/F	Epigastralgia	Stomach	Lung	SCC	7.9	9.1	3
					Adenocarcinoma	5.9	ND	3

SUV standardized uptake value, *ND* not done, *MFH* malignant fibrous histiocytoma, *SCC* squamous cell carcinoma, *M* male, *F* female

which metastases were found in the gastrointestinal tract were reviewed (men/women 3:1, age 63–78 years, mean 72 years).

FDG-PET imaging was performed as follows: an ECAT EXACT HR 47 PET camera (Siemens/CTI) was used, and imaging was performed using 3D acquisition at 60 min (all patients) and 120 min (two patients) after the intravenous administration of 250 MBq F-18-FDG. The collected data were reconstructed in a 128 × 128 pixel image matrix. The tissue attenuation of annihilation photons was corrected by transmission scans using rotating $^{68}Ge/^{68}Ga$ line sources. Six bed positions of the body trunk were used, which covered areas from the neck to the pelvis. The total time for one bed position was 6 min, with a transmission scan of 2 min and an emission scan of 4 min. The patient fasted for at least 6 h prior to the examination. Normal glucose level was confirmed prior to the PET scan. Regional FDG uptake in the affected area was expressed as standardized uptake value.

Table 1 summarizes the clinical and FDG-PET data of the four cases.

Case reports

Case 1

A 78-year-old man who had been diagnosed with lung adenocarcinoma by transbronchial lung biopsy received chemotherapy and achieved complete remission (CR). After 6 months, he sought medical attention with a chief complaint of vomiting. Computed tomography (CT) was performed and revealed a thickened wall and masses in the duodenum and jejunum (Fig. 1a). After 5 days, FDG-PET was performed for restaging and for the detection of metastatic lesions. FDG-PET showed hypermetabolism in the duodenum and jejunum (Fig. 1b), and in delayed scan showed increased uptake in the duodenum and jejunum. Gastroduodenoscopy showed a submucosal tumor in the duodenum. Metastatic adenocarcinoma was diagnosed by biopsy from the duodenum (Fig. 1c).

Case 2

A 76-year-old man who underwent surgery for malignant fibrous histiocytoma (MFH) of the femoral bone experienced gastrointestinal bleeding after 7 months, and was hospitalized. Hematological examination detected anemia, but no abnormality was found in the blood chemistry on admission. FDG-PET was performed to investigate metastasis. FDG-PET revealed hypermetabolic areas in the regions above the rectum (Fig. 2a), whereas colonoscopy showed a submucosal tumor in the rectum. The tumors were diagnosed as metastases from MFH of the femoral bone, and tumorectomy of the rectum was performed. The diagnosis was established histopathologically(Fig. 2b).

Case 3

A 63-year-old man had undergone surgery for squamous cell carcinoma (SCC) in the right upper lung field. Five years later, he had abdominal discomfort and a high carcinoembryonic (CEA) level (28.5 ng/ml). CT showed a round thickened wall in the stomach (Fig. 3a). After 10 days, FDG-PET performed for the detection of recurrent and metastatic lesions revealed hypermetabolism in the stomach (Fig. 3b). Gastroduodenoscopy showed a submucosal tumor of the stomach. Gastrectomy was performed and the tumor was histopathologically diagnosed as metastatic poorly differentiated SCC of the stomach (Fig. 3c).

Discussion

Metastatic tumors of the gastrointestinal tract rarely present with symptoms peculiar to these tumors, and are

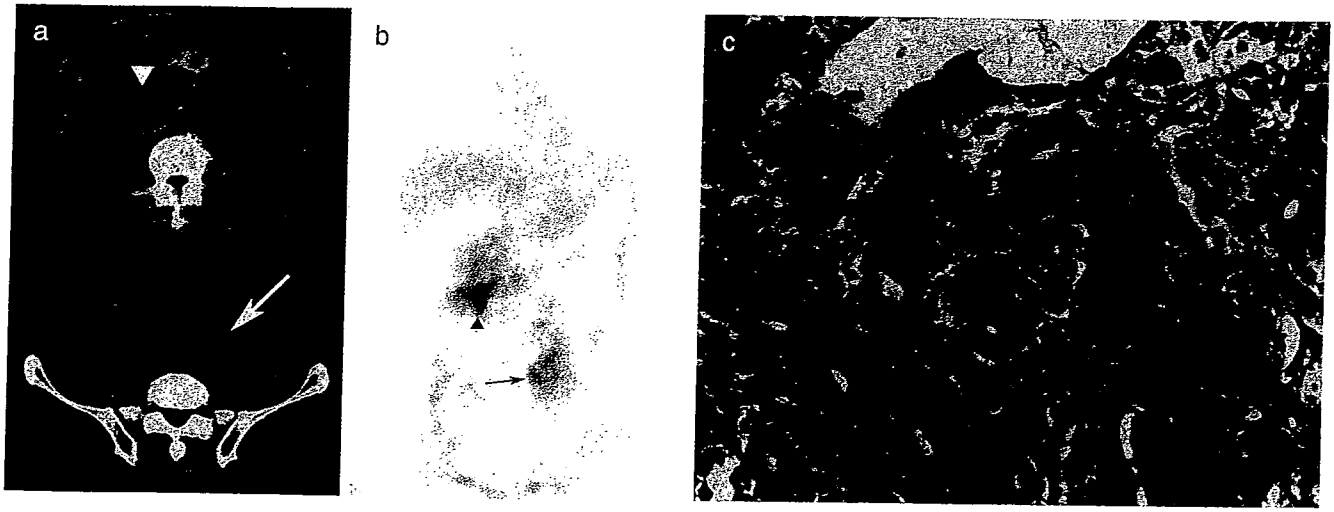

Fig. 1 Computed tomography revealed thickened wall and masses in the duodenum (*arrowhead*) and jejunum (*arrow*) (**a**). Fluorodeoxyglucose positron emission tomography (FDG-PET) showed hypermetabolism in the duodenum (*arrowhead*) and jejunum (*arrow*) (**b**). Pathology by biopsies from the duodenum (hematoxylin-eosin, H&E) (**c**) revealed findings similar to those of pathological tissue of lung carcinoma obtained by biopsy from transbronchial lung biopsy, confirming a metastatic adenocarcinoma

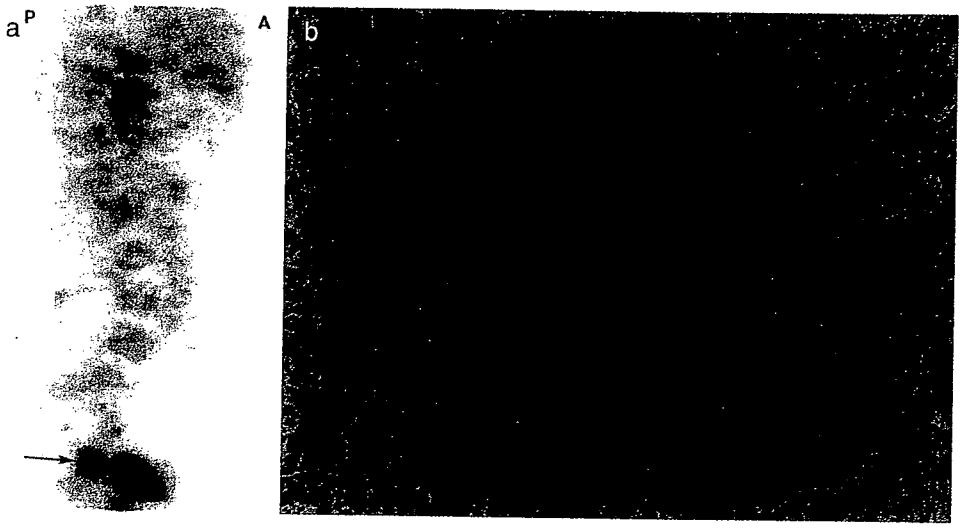

Fig. 2 FDG-PET showing hypermetabolism in the rectum (*arrowhead*) (**a**). The mean standardized uptake value calculated by FDG-PET was 5.1 for the rectal tumor. Pathology by surgery from the rectum (H&E) confirmed a metastatic malignant fibrous histiocytoma (**b**)

rarely detected before the development of serious complications such as acute abdomen. Abrams et al. [1] reported that they found metastases to the stomach and intestine and esophagus in 20% and 3.1% of the 1000 autopsies of cancer patients. Meyers and McSweeney [9] reported that the primary lesions of metastatic tumors of the gastrointestinal tract in 40 clinical patients were malignant melanoma (57%), breast cancer (25%), and lung cancer (18%), indicating that malignant melanoma is the most frequent, followed by breast and lung cancers. Metastatic tumors of the gastrointestinal tract often present with abdominal pain, vomiting, anemia, and melena, and often have metastasized to other organs at the time of detection [10]. Sometimes they first present with acute abdomen such as intestinal perforation, intussusception, intestinal obstruction, or massive gastrointestinal bleeding [3, 11, 12]. Hence, it is desirable to detect metastatic tumors of the gastrointestinal tract before the development of such serious complications. The role and potential value of FDG-PET scanning in certain neoplasms have been widely investigated in recent years [4, 5]. These investigations have been performed predominantly on lung, colorectal, breast, and brain tumors. More recently, the role of FDG-PET has been in upper gastrointestinal neoplasms [4–6, 13, 14]. The usefulness of FDG-PET in recurrent tumors other than these primary tumors of the esophagus, stomach, and intestine has also reported [15, 16], encouraging expectations that FDG-PET will also be useful for the detection of metastatic tumors of the gastrointestinal tract. A few

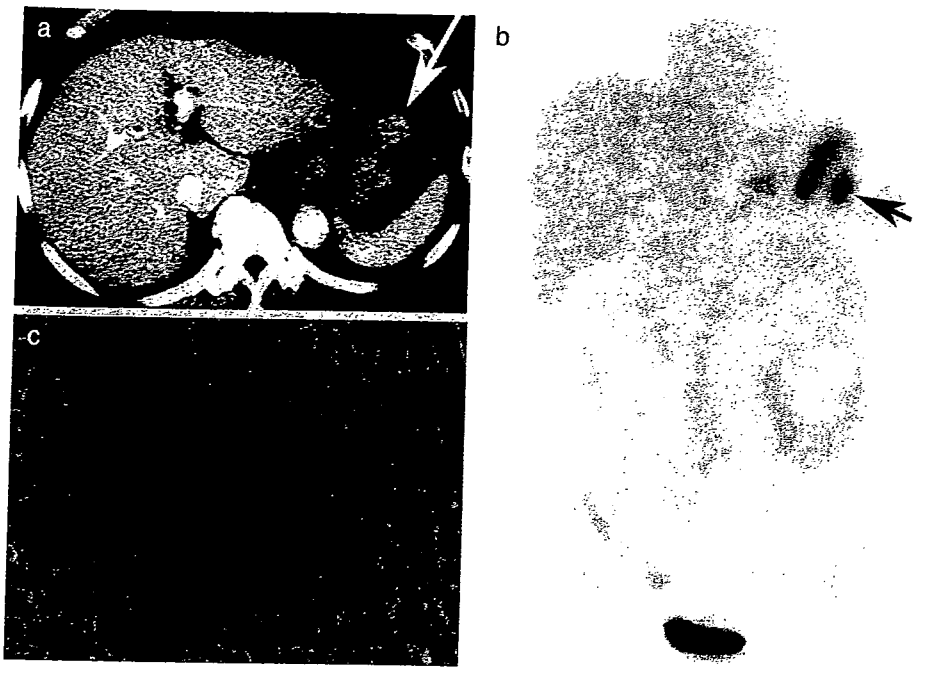

Fig. 3 Computed tomography showed a round mass in the stomach (*arrow*) (a). FDG-PET shows hypermetabolism in the stomach (*arrow*) (b). Pathological examination of specimens obtained by surgery from the stomach (H&E) (c) revealed findings similar to those of pulmonary carcinoma obtained from the lung at surgery, confirming a metastatic poorly differentiated squamous cell carcinoma

studies have reported metastatic tumors of the gastrointestinal tract and the use of FDG-PET in gastrointestinal metastases [17, 18]. Studies have reported on 124 patients with gastrointestinal metastasis from lung cancer, 106 of whom were diagnosed on the occasion of serious complications such as perforation [3, 19]. Among our patients with lung cancer and MFH, one patient with vomiting after CR for chemotherapy, two patients with increased levels of CEA, and one patient with gastrointestinal bleeding underwent FDG-PET for the detection of recurrent lesions, which showed FDG uptake for the detection of gastrointestinal tract and other recurrent lesions. Thus, FDG-PET enabled the detection of metastatic tumors before the development of serious complications, and CT demonstrated well the local anatomy of the metastatic tumor of the gastrointestinal tract and other recurrent lesions.

FDG-PET imaging provided valuable information for the diagnosis of gastrointestinal metastasis, and these observations suggest that this imaging modality is also useful for the detection of metastatic tumors of the gastrointestinal tract, thereby enabling the prevention of complications such as intestinal obstruction, and massive bleeding, caused by metastatic tumors of the gastrointestinal tract.

References

1. Abrams HL, Spiro R, Goldstein N. Metastasis in carcinoma: analysis of 1000 autopsied cases. Cancer 1950;3:74–85.
2. Menuck LS, Amberg JR. Metastatic disease involving the stomach. Am J Dig Dis 1975;20:903–13.
3. Garwood RA, Sawyer MD, Ledesma EJ, Foley E, Claridge JA. A case and review of bowel perforation secondary to metastatic lung cancer. Am Surg 2005;71:110–6.
4. Kostakoglu L, Agress H, Golodsmith FS. Clinical role of FDG PET in evaluation of cancer patients. Radiographics 2003;23:315–40.
5. Rohren EM, Turkington TG, Coleman RE. Clinical applications of PET in oncology. Radiology 2004;231:305–31.
6. van Kouwen MC, Oyen WJ, Negengast FM, Jansen JB, Drenth JP. FDG-PET scanning in the diagnosis of gastrointestinal cancers. Scan J Gastroenterol Suppl 2004;241:85–92.
7. Gutman F, Albeirni JL, Wartski M, Vilain D, LeStanc E, Sarandi F, et al. Incidental colonic focal lesion detected by FDG PET/CT. Am J Roentgenol 2005;185:495–500.
8. Hustrinx R. PET imaging in assessing gastrointestinal tumors. Radiol Clin North Am 2004;42:1123–39.
9. Meyers MA, McSweeney J. Secondary neoplasms of the bowel. Radiology 1972;105:1–11.
10. Hinoshita E, Nakahashi H, Wakasugi K, Kaneko S, Hamatake M, Sugimachi K. Duodenal metastasis from large cell carcinoma of the lung: report of a case. Surg Today 1999; 29:799–802.
11. De Castro CA, Dockerty MB, Mayo CW. Metastatic tumors of the small intestines. Surg Gynecol Obstet 1957;105:159–65.
12. Nussbaum M, Grossman M. Metastasis to the esophagus causing gastrointestinal bleeding. Am J Gastroenterol 1976;66:467–72.
13. McAteer D, Wallis F, Couper G, Norton M, Welch A, Bruced D, et al. Evaluation of F18-FDG positron emission tomography in gastric and esophageal carcinoma. Br J Radiol 1999;72:525–9.
14. Chen J, Cheong JH, Yun MJ, Kim J, Lim JS, Hyung WJ, et al. Improvement in preoperative staging of gastric adenocarcinoma with positron emission tomography. Cancer 2005;103:2283–90.

15. Choi MY, Lee KM, Chung JK, Lee DS, Jeong JM, Park JG, et al. Correlation between by FDG PET in postoperative patients with recurrent colorectal cancer. Ann Nucl Med 2005;19:123–9.
16. Kato H, Miyazaki T, Nakajima M, Fukuchi M, Manda R, Kuwano H. Value of positron emission tomography in the diagnosis of recurrent oesophageal carcinoma. Br J Surg 2004;91:1004–9.
17. Alibazoglu H, Alibazoglu B, Ali A, La Monica G. False-negative FDG-PET imaging in a patient with metastatic melanoma and ileal intussusception. Clin Nucl Med 1999; 24:129.
18. Tatlidil R, Mandelker NM. FDG-PET in the detection of gastrointestinal metastases in melanoma. Melanoma Res 2001;11:297–301.
19. Yamamoto M, Matsuzaki K, Kusumoto H, Uchida H, Mine H, Kabashima A, et al. Gastric metastasis from lung carcinoma: case report. Hepatogastroenterology 2002;49:363-5.

Available online at www.sciencedirect.com
ScienceDirect
Prostaglandins, Leukotrienes and Essential Fatty Acids 77 (2007) 187–193
Prostaglandins Leukotrienes & Essential Fatty Acids
www.elsevier.com/locate/plefa

Platelet-derived growth factor-BB amplifies $PGF_{2\alpha}$-stimulated VEGF synthesis in osteoblasts: Function of phosphatidylinositol 3-kinase

Haruhiko Tokuda[a,b], Shinji Takai[b], Yoshiteru Hanai[a,b], Atsushi Harada[c], Rie Matsushima-Nishiwaki[b], Shigeru Akamatsu[d], Toshiki Ohta[e], Osamu Kozawa[b,*]

[a]*Department of Clinical Laboratory, National Hospital for Geriatric Medicine, National Center for Geriatrics and Gerontology, Obu, Aichi 474 8511, Japan*
[b]*Department of Pharmacology, Gifu University Graduate School of Medicine, Gifu 501 1194, Japan*
[c]*Functional Restoration, National Hospital for Geriatric Medicine, National Center for Geriatrics and Gerontology, Obu, Aichi 474 8511, Japan*
[d]*Critical Care Center, Matsunami General Hospital, Kasamatsu, Gifu 501 6062, Japan*
[e]*Internal Medicine, National Hospital for Geriatric Medicine, National Center for Geriatrics and Gerontology, Obu, Aichi 474 8511, Japan*

Received 9 November 2006; received in revised form 2 July 2007; accepted 2 October 2007

Abstract

We have reported that prostaglandin $F_{2\alpha}$ ($PGF_{2\alpha}$) stimulates the synthesis of vascular endothelial growth factor (VEGF) via p44/p42 mitogen-activated protein (MAP) kinase in osteoblast-like MC3T3-E1 cells. In addition, we recently showed that phosphatidylinositol 3 (PI3)-kinase activated by platelet-derived growth factor-BB (PDGF-BB) negatively regulates the interleukin-6 synthesis in these cells. In the present study, we investigated the effect of PDGF-BB on the $PGF_{2\alpha}$-induced VEGF synthesis in MC3T3-E1 cells. PDGF-BB, which alone did not affect the levels of VEGF, significantly enhanced the $PGF_{2\alpha}$-stimulated VEGF synthesis. The amplifying effect of PDGF-BB was dose dependent in the range between 10 and 70 ng/ml. LY294002 or wortmannin, specific inhibitors of PI3-kinase, which by itself failed to affect the $PGF_{2\alpha}$-stimulated VEGF synthesis, significantly suppressed the amplification by PDGF-BB. PD98059, a specific inhibitor of MEK1/2, suppressed the amplification by PDGF-BB of the $PGF_{2\alpha}$-stimulated VEGF synthesis similar to the levels of $PGF_{2\alpha}$ with PD98059. PDGF-BB itself induced the phosphorylation of p44/p42 MAP kinase in these cells, and the effects of PDGF-BB and $PGF_{2\alpha}$ on the phosphorylation of p44/p42 MAP kinase were additive. Moreover, LY294002 had little effect on the phosphorylation of p44/p42 MAP kinase induced by $PGF_{2\alpha}$ with PDGF-BB. These results strongly suggest that $PGF_{2\alpha}$-stimulated VEGF synthesis is amplified by PI3-kinase-mediating PDGF-BB signaling in osteoblasts, and that the effect is exerted at a point downstream from p44/p42 MAP kinase.

1. Introduction

Platelet-derived growth factor (PDGF) is a mitogenic polypeptide, which mainly acts on connective tissue cells [1,2]. PDGF occurs as five different isoforms [2]. PDGF isoforms were initially isolated from human platelets, but have been shown to be synthesized and released from a variety of cell types including osteosarcoma and osteoblasts [1,3,4]. It is well recognized that bone metabolism is strictly regulated by two functional cells, osteoblasts and osteoclasts, responsible for bone formation and bone resorption, respectively [5]. As for bone metabolism, PDGF-BB is a potent stimulator of osteoblast proliferation and induces bone resorption [4]. It is recognized that PDGF, released during platelet aggregation, plays a crucial role in fracture healing as a systemic factor and that PDGF also regulates bone remodeling as a local factor [4]. PDGF receptor has an intrinsic protein tyrosine kinase activity and associates with SH-2 domain-containing substrates such as phospholipase C-γ and phosphatidylinositol 3-kinase (PI3-kinase) [1]. We have previously reported that

*Corresponding author. Tel.: +81 58 230 6214; fax: +81 58 230 6215.
E-mail address: okozawa@gifu-u.ac.jp (O. Kozawa).

0952-3278/$ - see front matter © 2007 Elsevier Ltd. All rights reserved.
doi:10.1016/j.plefa.2007.10.001

PDGF-BB activates phosphatidylcholine-hydrolyzing phospholipase D via tyrosine kinase activation, resulting in protein kinase C activation in osteoblast-like MC3T3-E1 cells [6]. In addition, we recently showed that PI3-kinase negatively regulates the PDGF-BB-stimulated interleukin-6 synthesis in these cells [7]. However, the exact role of PDGF-BB in osteoblasts has not yet been fully clarified.

Bone remodeling carried out by osteoclasts and osteoblasts is accompanied with new capillaries extending [8,9]. During bone remodeling, capillary endothelial cells provide the microvasculature. Therefore, it is well recognized that the activities of osteoblasts, osteoclasts, and capillary endothelial cells are closely coordinated and regulate bone metabolism [10]. These functional cells are considered to influence one another via humoral factors as well as by direct cell-to-cell contact. Vascular endothelial growth factor (VEGF) is an angiogenic growth factor displaying high specificity for vascular endothelial cells [11]. VEGF that is synthesized and secreted from a variety of cell types such as vascular smooth muscle cells, increases capillary permeability and stimulates proliferation of endothelial cells [11]. As for bone metabolism, it has been shown that inactivation of VEGF causes complete suppression of blood vessel invasion concomitant with impaired trabecular bone formation and expansion of hypertrophic chondrocyte zone in mouse tibial epiphyseal growth plate [12]. Accumulating evidence suggests that osteoblasts among bone cells synthesize and secrete VEGF in response to various physiological agents [11,13–15]. We have previously reported that $PGF_{2\alpha}$ (prostaglandin $F_{2\alpha}$) stimulates VEGF synthesis in MC3T3-E1 cells, and that among the mitogen-activated protein (MAP) kinase superfamily [16], p44/p42 MAP kinase plays as a positive regulator in the VEGF synthesis [17]. Taking these findings into account, it is currently speculated that VEGF secreted from osteoblasts may play an important role in the regulation of bone metabolism [10,18]. However, the mechanism behind VEGF synthesis and its synthesis in osteoblasts is not fully understood.

In the present study, we investigated the effect of PDGF-BB on the $PGF_{2\alpha}$-stimulated VEGF synthesis in osteoblast-like MC3T3-E1 cells. We here show that PDGF-BB up-regulates $PGF_{2\alpha}$-stimulated VEGF synthesis via PI3-kinase in these cells.

2. Materials and methods

2.1. Materials

$PGF_{2\alpha}$ was purchased form Sigma Chemical Co. (St. Louis, MO). PDGF-BB and mouse VEGF enzyme immunoassay kit were purchased from R&D Systems, Inc. (Minneapolis, MN). LY294002, wortmannin and PD98059 were obtained from Calbiochem–Novabiochem Co. (La Jolla, CA). Phospho-specific PI3-kinase antibodies, PI3-kinase antibodies, phosphor-specific p44/p42 MAP kinase antibodies and p44/p42 MAP kinase antibodies were purchased from Cell Signaling Technology (Beverly, MA). ECL Western blotting detection system was purchased from Amersham Biosciences (Piscataway, NJ). Other materials and chemicals were obtained from commercial sources. $PGF_{2\alpha}$, was dissolved in ethanol. LY294002, wortmannin and PD98059 were dissolved in dimethyl sulfoxide (DMSO). The maximum concentration of ethanol or DMSO was 0.1%, which did not affect the assay for VEGF or the Western blotting analysis.

2.2. Cell culture

Cloned osteoblast-like MC3T3-E1 cells derived from newborn mouse calvaria [19] were maintained as previously described [20]. Briefly, the cells were cultured in α-minimum essential medium (α-MEM) containing 10% fetal calf serum (FCS) at 37 °C in a humidified atmosphere of 5% CO_2/95% air. The cells were seeded into 35-mm (5×10^4) or 90-mm (5×10^5) diameter dishes in α-MEM containing 10% FCS. After 5 days, the medium was exchanged for α-MEM containing 0.3% FCS. The cells were used for experiments after 48 h.

2.3. VEGF assay

The cultured cells were stimulated by various dose of $PGF_{2\alpha}$ in 1 ml of α-MEM containing 0.3% FCS for the indicated periods. When indicated, the cells were pretreated with LY294002, wortmannin or PD98059 for 60 min. The conditioned medium was collected at the end of the incubation, and the VEGF concentration was measured by ELISA kit.

2.4. Analysis of Western blotting

The cultured cells were stimulated by $PGF_{2\alpha}$ and/or PDGF-BB in α-MEM containing 0.3% FCS for the indicated periods. The cells were washed twice with phosphate-buffered saline and then lysed, homogenized and sonicated in a lysis buffer containing 62.5 mM Tris/HCl, pH 6.8, 2% sodium dodecyl sulfate (SDS), 50 mM dithiothreitol and 10% glycerol. The cytosolic fraction was collected as a supernatant after centrifugation at $125{,}000 \times g$ for 10 min at 4 °C. SDS-polyacrylamide gel electrophoresis (PAGE) was performed by Laemmli [21] in 10% polyacrylamide gel. A Western blotting analysis was performed as described previously [17] by using phospho-specific p44/p42 MAP kinase antibodies, p44/p42 MAP kinase antibodies, phospho-specific PI3-kinase antibodies or PI3-kinase antibodies with

peroxidase-labeled antibodies raised in goat against rabbit IgG being used as second antibodies. The peroxidase activity on PVDG membrane was visualized on X-ray film by means of the ECL Western blotting detection system. When indicated, the cells were pretreated with various doses of LY294002 or wortmannin for 60 min.

2.5. Determination

The absorbance of enzyme immunoassay samples was measured at 450 nm with EL 340 Bio Kinetic Reader (Bio-Tek Instruments, Inc., Winooski, VT). The densitometric analysis was performed using Molecular Analyst/Macintosh (Bio-Rad Laboratories, Hercules, CA).

2.6. Statistical analysis

The data were analyzed by ANOVA followed by the Bonferroni method for multiple comparisons between pairs and a $p<0.05$ was considered significant. All data are presented as the mean ± S.E.M. of triplicate determinations. Each experiment was repeated three times with similar results.

3. Results

3.1. Effect of PDGF-BB on $PGF_{2\alpha}$-induced VEGF synthesis in MC3T3-E1 cells

PDGF-BB, which alone had no effect on the VEGF levels, significantly enhanced the $PGF_{2\alpha}$-stimulated VEGF synthesis in a time-dependent manner in osteoblast-like MC3T3-E1 cells (Fig. 1). The effect of PDGF-BB was dose-dependent in the range between 10 and 70 ng/ml (Fig. 2). The maximum effect of PDGF-BB on the VEGF synthesis was observed at 70 ng/ml, which caused about 16 times enhancement of the-$PGF_{2\alpha}$-effect.

3.2. Effect of LY294002 or wortmannin on the amplification by PDGF-BB of the $PGF_{2\alpha}$-induced VEGF synthesis in MC3T3-E1 cells

We have previously reported that PI3-kinase activated by PDGF-BB limits the PDGF-BB-stimulated IL-6 synthesis in osteoblast-like MC3T3-E1 cells [7]. In order to investigate whether the amplifying effect of PDGF-BB on the $PGF_{2\alpha}$-stimulated VEGF synthesis is via activation of PI3-kinase in MC3T3-E1 cells, we next examined the effect of LY294002, a specific inhibitor of PI3-kinase [22], on the synthesis of VEGF. LY294002, which by itself did not suppress the $PGF_{2\alpha}$-induced VEGF synthesis, significantly reduced the enhancement

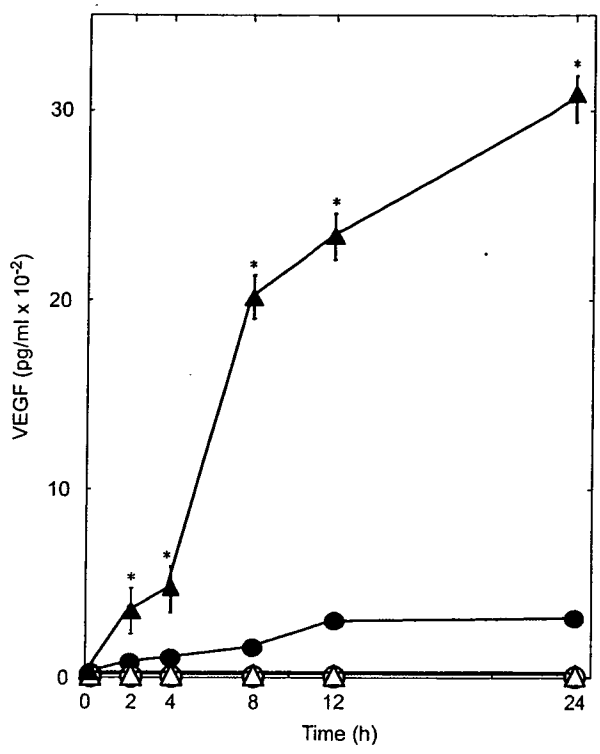

Fig. 1. Effect of PDGF-BB on the $PGF_{2\alpha}$-stimulated VEGF synthesis in MC3T3-E1 cells. The cultured cells were pretreated with 30 ng/ml PDGF-BB (▲, △) or vehicle (●, ○) for 60 min, and then stimulated by 10 μM $PGF_{2\alpha}$ (●, ▲) or vehicle (○, △) for the indicated periods. Each value represents the mean ± SEM of triplicate determinations. Similar results were obtained with two additional and different cell preparations. *$p<0.05$, compared to the value of $PGF_{2\alpha}$ alone.

by PDGF-BB of $PGF_{2\alpha}$-induced VEGF synthesis (Table 1). The effect of LY294002 was dose dependent in the range between 1 and 50 μM (data not shown).

Wortmannin, another PI3-kinase inhibitor [23], as well as LY294002, also suppressed the amplification by PDGF-BB of the VEGF synthesis without affecting the $PGF_{2\alpha}$-stimulated synthesis (Table 2). The effect of wortmannin was dose dependent between 10 and 30 μM (data not shown). We also examined the effects of LY294002 or wortmannin on the PDGF-BB-induced phosphorylation of PI3-kinase in these cells. Neither LY294002 nor wortmannin inhibited PDGF-BB-induced phosphorylation of PI3-kinase in these cells (Fig. 3).

3.3. Effect of PD98059 on the amplification by PDGF-BB of the $PGF_{2\alpha}$-induced VEGF synthesis in MC3T3-E1 cells

In a previous study [17], we showed that $PGF_{2\alpha}$ stimulates VEGF synthesis through p44/p42 MAP kinase activation in osteoblast-like MC3T3-E1 cells. In order to clarify whether the up-regulating effect of PDGF-BB on $PGF_{2\alpha}$-induced VEGF synthesis is due to p44/p42 MAP kinase activation in MC3T3-E1 cells, we

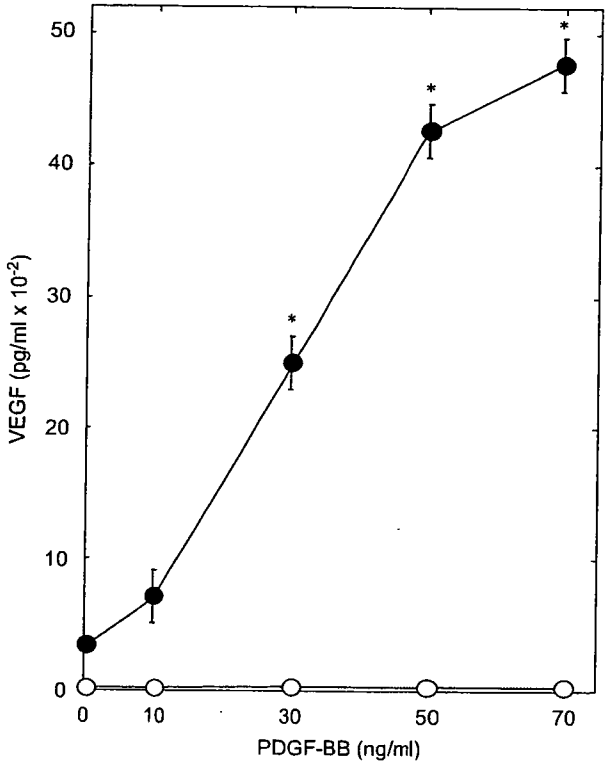

Fig. 2. Dose dependent effect of PDGF-BB on the $PGF_{2\alpha}$-stimulated VEGF synthesis in MC3T3-E1 cells. The cultured cells were pretreated with various doses of PDGF-BB for 60 min, and then stimulated by 10 μM $PGF_{2\alpha}$ (●) or vehicle (○) for 24 h. Each value represents the mean ± SEM of triplicate determinations. Similar results were obtained with two additional and different cell preparations. $^{*}p<0.05$, compared to the value of $PGF_{2\alpha}$ alone.

Table 1
Effect of LY294002 on the enhancement by PDGF-BB of the $PGF_{2\alpha}$-stimulated VEGF synthesis in MC3T3-E1 cells

LY294002	PDGF-BB	$PGF_{2\alpha}$	VEGF (pg/ml)
–	–	–	15 ± 5
–	–	+	306 ± 27*
–	+	–	20 ± 5
–	+	+	3919 ± 157**
+	–	–	10 ± 5
+	–	+	440 ± 45
+	+	–	23 ± 10
+	+	+	1381 ± 88***

The cultured cells were pretreated with 50 μM LY294002 or vehicle for 60 min and then incubated by 30 ng/ml PDGF-BB or vehicle for 60 min. The cells were stimulated by 10 μM $PGF_{2\alpha}$ or vehicle for 48 h. Each value represents the mean ± SEM of triplicate determinations. Similar results were obtained with two additional and different cell preparations.

$^{*}p<0.05$, compared to the control.

$^{**}p<0.05$, compared to the value of $PGF_{2\alpha}$ alone.

$^{***}p<0.05$, compared to the value of $PGF_{2\alpha}$ with PDGF-BB pretreatment.

Table 2
Effects of wortmannin or PD98059 on the enhancement by PDGF-BB of the $PGF_{2\alpha}$-stimulated VEGF synthesis in MC3T3-E1 cells

Inhibitor	PDGF-BB	$PGF_{2\alpha}$	VEGF (pg/ml)
–	–	–	20 ± 5
–	–	+	370 ± 28*
–	+	–	15 ± 10
–	+	+	3010 ± 139**
Wortmannin	–	–	20 ± 5
Wortmannin	–	+	462 ± 45
Wortmannin	+	–	18 ± 10
Wortmannin	+	+	406 ± 36***
PD98059	–	–	18 ± 5
PD98059	–	+	114 ± 20**
PD98059	+	–	15 ± 8
PD98059	+	+	122 ± 25***

The cultured cells were pretreated with 30 nM wortmannin, 30 μM PD98059 or vehicle for 60 min and then incubated by 30 ng/ml PDGF-BB or vehicle for 60 min. The cells were stimulated by 10 μM $PGF_{2\alpha}$ or vehicle for 24 h. Each value represents the mean ± SEM of triplicate determinations. Similar results were obtained with two additional and different cell preparations.

$^{*}p<0.05$, compared to the control.

$^{**}p<0.05$, compared to the value of $PGF_{2\alpha}$ alone.

$^{***}p<0.05$, compared to the value of $PGF_{2\alpha}$ with PDGF-BB pretreatment.

examined the effect of PD98059, a specific inhibitor of the upstream kinase that activates p44/p42 MAP kinase [24], on the enhancement by PDGF-BB. PD98059, which by itself had no effect on the basal levels of VEGF, significantly reduced the enhancement by PDGF-BB of $PGF_{2\alpha}$-induced VEGF synthesis to the levels of the $PGF_{2\alpha}$ with PD98059 (Table 2). The effect of PD98059 was dose dependent in the range between 1 and 30 μM (data not shown).

3.4. Effect of PDGF-BB in combination with $PGF_{2\alpha}$ on the phosphorylation of p44/p42 MAP kinase in MC3T3-E1 cells

We further investigated whether PDGF-BB could enhance the phosphorylation of p44/p42 MAP kinase induced by $PGF_{2\alpha}$ in osteoblast-like MC3T3-E1 cells, and whether LY294002 could abolish it in osteoblast-like MC3T3-E1 cells. PDGF-BB itself induced the phosphorylation of p44/p42 MAP kinase in these cells, and that the effects of PDGF-BB and $PGF_{2\alpha}$ on the phosphorylation of p44/p42 MAP kinase were additive (Fig. 4). In addition, LY294002 had little effect on the phosphorylation of p44/p42 MAP kinase induced by $PGF_{2\alpha}$ with PDGF-BB (Fig. 4).

4. Discussion

In the present study, we showed that PDGF-BB, which alone did not affect the levels of VEGF,

significantly amplified the $PGF_{2\alpha}$-stimulated VEGF synthesis in osteoblast-like MC3T3-E1 cells. We next investigated the mechanism of PDGF-BB behind the amplification. In our previous study [7], we reported that PDGF-BB- activated PI3-kinase negatively regulates the interleukin-6 synthesis in MC3T3-E1 cells. We investigated whether or not PI3-kinase functions in the PDGF-BB-enhanced VEGF synthesis in osteoblast-like MC3T3-E1 cells. LY294002, a specific inhibitor of PI3-kinase [22], markedly suppressed the amplification by PDGF-BB of $PGF_{2\alpha}$-induced VEGF synthesis while the $PGF_{2\alpha}$-induced VEGF synthesis was not inhibited by LY294002. Thus, these results suggest that PI3-kinase is implicated in the PDGF-BB-induced potentiation. In addition, wortmannin, another PI3-kinase inhibitor [23], reduced the PDGF-BB-effect in the VEGF synthesis without suppressing the $PGF_{2\alpha}$-induced VEGF synthesis as well as LY294002. We found that neither LY294002 nor wortmannin could inhibit PDGF-BB-induced phosphorylation of PI3-kinase in these cells. Both LY294002 and wortmannin are competitive inhibitors of PI3-kinase [22,23]. It is well recognized that PI3-kinase is activated by its phosphorylation and that LY294002 is a highly selective PI3-kinase inhibitor which blocks PI3-kinase-dependent phosphorylation of its target proteins [22]. Namely, LY294002 and wortmannin are not inhibitors of the phosphorylation of PI3-kinase. Thus, it is reasonable that the effects of these inhibitors on PI3-kinase-mediating PDGF-BB signaling are exerted at a point downstream of the phosphorylation of PI3-kinase in MC3T3-E1 cells. Indeed, we have previously reported that the phosphorylation of Akt induced by PDGF-BB is significantly inhibited by both LY294002 and wortmannin [25]. Therefore, it is sure that these inhibitors attenuate the PDGF-BB-activating PI3-kinase/Akt signaling in these cells. On the other hand, the amplification by PDGF-BB of $PGF_{2\alpha}$ was observed during 4 and 8 h in the time course study. It is possible that PDGF-BB-stimulated other protein synthesis might be involved in the PDGF-BB effect. Therefore, taking our results into account as a whole, it is most likely that PDGF-BB activates the PI3-kinase pathway, resulting in the potentiation of $PGF_{2\alpha}$-induced VEGF synthesis in MC3T3-E1 cells.

It is well recognized that the MAP kinase superfamily mediates intracellular signaling of extracellular agonists and plays a pivotal role in cellular functions including

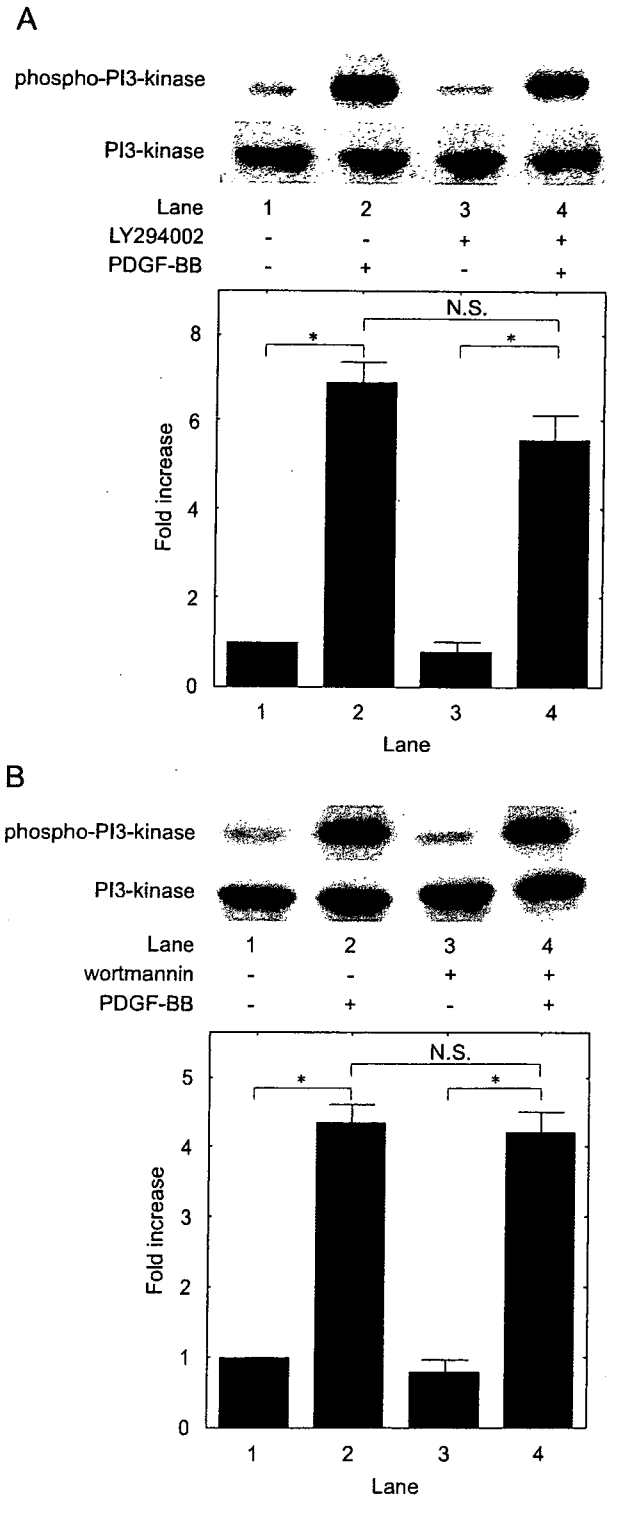

Fig. 3. Effects of LY294002 or wortmannin on the phosphorylation of PI3-kinase induced by PDGF-BB in MC3T3-E1 cells. The cultured cells were pretreated with 50 μM LY294002 (A), 30 nM wortmannin (B) or vehicle for 60 min, and then stimulated by 30 ng/ml PDGF-BB or vehicle for 60 min. The extracts of the cells were subjected to SDS-PAGE with a subsequent Western blotting analysis with antibodies against phospho-specific PI-3 kinase or PI-3 kinase. The histogram shows quantitative representations of the levels of PDGF-BB-induced phosphorylation obtained from a laser densitometric analysis of three independent experiments. Each value represents the mean ± SEM of triplicate determinations. Similar results were obtained with two additional and different cell preparations. $*p < 0.05$, compared to the value of control. N.S., no statistical significance.

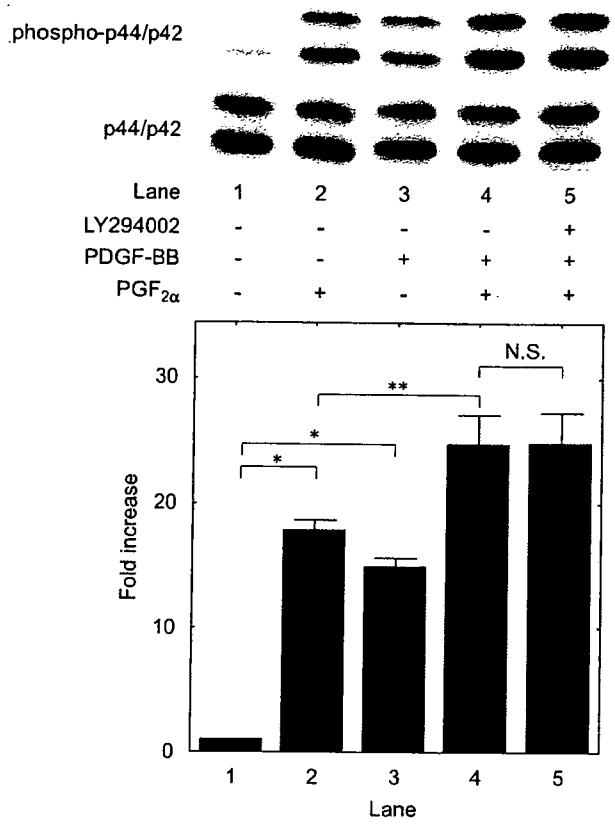

Fig. 4. Effect of PDGF-BB in combination with $PGF_{2\alpha}$ on the phosphorylation of p44/p42 MAP kinase in MC3T3-E1 cells. The cultured cells were pretreated with 50 μM LY294002 or vehicle for 60 min, and then incubated by 30 ng/ml PDGF-BB or vehicle for 60 min. The treated cells were stimulated by 10 μM $PGF_{2\alpha}$ or vehicle for 30 min. The extracts of cells were subjected to SDS-PAGE with subsequent Western blotting analysis with antibodies against phospho-specific p44/p42 MAP kinase or p44/p42 MAP kinase. The histogram shows quantitative representations of the levels of PDGF-BB- and/or $PGF_{2\alpha}$-induced phosphorylation obtained from a laser densitometric analysis of three independent experiments. Each value represents the mean ± SEM of triplicate determinations. Similar results were obtained with two additional and different cell preparations. $*p<0.05$, compared to the value of control. $**p<0.05$, compared to the value of $PGF_{2\alpha}$ alone. N.S., no statistical significance.

proliferation, differentiation, and apoptosis in a variety of cells [16]. Three major MAP kinase, p44/p42 MAP kinase, p38 MAP kinase, and SAPK/JNK are known as central elements used by mammalian cells to transducer the diverse messages [16]. In our previous study [17], we have shown that p44/p42 MAP kinase acts as a positive regulator in $PGF_{2\alpha}$-induced VEGF synthesis in MC3T3-E1 cells. Therefore, we tried to clarify the relationship between PDGF-BB-effect and p44/p42 MAP kinase in the $PGF_{2\alpha}$-stimulated VEGF synthesis in these cells. The amplification by PDGF-BB of the $PGF_{2\alpha}$-stimulated VEGF synthesis was suppressed by PD98059, a specific inhibitor of MEK1/2 [23], similar to the levels of $PGF_{2\alpha}$ with PD98059. Moreover, we found that PDGF-BB itself induced the phosphorylation of p44/p42 MAP kinase in these cells, and that the effects of PDGF-BB and $PGF_{2\alpha}$ on the phosphorylation of p44/p42 MAP kinase were additive. These results suggest that PDGF-BB activates p44/p42 MAP kinase independently from $PGF_{2\alpha}$ in these cells. PDGF-BB as well as $PGF_{2\alpha}$ induced the phorphorylation of p44/p42 MAP kinase, however, VEGF synthesis was only observed by $PGF_{2\alpha}$, not by PDGF-BB. Our results indicate that PDGF-BB-induced p44/p42 MAP kinase activation alone is not sufficient for VEGF synthesis in osteoblasts, which is quite different from $PGF_{2\alpha}$-induced p44/p42 MAP kinase activation. In addition, the increase in VEGF by PDGF-BB and $PGF_{2\alpha}$ was not additive but synergistic. We also found that LY294002 had little effect on the phosphorylation of p44/p42 MAP kinase induced by $PGF_{2\alpha}$ with PDGF-BB. Therefore, it is probable that the enhancement by PDGF of $PGF_{2\alpha}$-induced VEGF synthesis through PI3-kinase is exerted at a point downstream from p44/p42 MAP kinase in these cells. As a whole, it is most likely that PDGF-BB independently activates p44/p42 MAP kinase and PI3-kinase in osteoblasts, and the latter is involved in the enhancement of $PGF_{2\alpha}$-induced VEGF synthesis at a point downstream from p44/p42 MAP kinase.

The expansion of capillary network providing microvasculature is an essential process of bone remodeling [10]. Since VEGF is a specific mitogen of vascular endothelial cells [11], it is recognized that VEGF secreted by osteoblasts plays a crucial role as an intercellular mediator between osteoblasts and vascular endothelial cells in bone metabolism. Moreover, it has been reported that VEGF is involved in trabecular bone formation and expansion of the hypertrophic chondrocyte zone in epiphyseal growth plate of mouse [12], supporting the significance of VEGF in bone metabolism. On the other hand, the mitogenic activities of PDGF and its release by platelets suggest a pivotal role in wound healing and bone fracture repair [26]. Therefore, our present findings lead us to speculate that PDGF-BB-enhanced VEGF synthesis from osteoblasts plays a pivotal role in the process of bone remodeling via up-regulating the proliferation of capillary endothelial cells. Further investigations are required to elucidate the precise role of PDGF-BB in bone metabolism.

In conclusion, our present results strongly suggest that PI3-kinase signaling pathway activated by PDGF-BB amplifies $PGF_{2\alpha}$-induced VEGF synthesis in osteoblasts, and that the effect is exerted at a point downstream from p44/p42 MAP kinase.

Acknowledgments

We are very grateful to Yoko Kawamura and Seiko Sakakibara for their skillful technical assistance. This

investigation was supported in part by Grant-in-Aid for Scientific Research (16590873 and 16591482) for the Ministry of Education, Science, Sports and Culture of Japan, the Research Grants for Longevity Sciences (15A-1, 15C-2 and 17A-3), Research on Proteomics and Research on Longevity Sciences from the Ministry of Health, Labour and Welfare of Japan.

References

[1] C.H. Heldin, B. Westermark, Mechanism of action and in vivo role of platelet-derived growth factor, Physiol. Rev. 79 (1999) 1283–1316.

[2] C.H. Heldin, U. Eriksson, A. Ostman, New members of the platelet-derived growth factor family of mitogens, Arch. Biochem. Biophys. 398 (2002) 284–290.

[3] C.H. Heldin, A. Johnsson, S. Wennergren, C. Wernstedt, C. Betsholtz, B. Westermark, A human osteosarcoma cell line secretes a growth factor structurally related to a homodimer of PDGF A-chains, Nature 319 (1986) 511–514.

[4] E. Canalis, S. Rydziel, Platelet-derived growth factor and the skeleton, Principles Bone Biol. 2 (2002) 817–824.

[5] P.J. Nijweide, E.H. Burger, J.H.M. Feyen, Cells of bone: proliferation, differentiation, and hormonal regulation, Physiol. Rev. 86 (1986) 855–886.

[6] O. Kozawa, A. Suzuki, Y. Watanabe, J. Shinoda, Y. Oiso, Effect of platelet-derived growth factor on phosphatidylcholine-hydrolyzing phospholipase D in osteoblast-like cells, Endocrinology 136 (1995) 4473–4478.

[7] Y. Hanai, H. Tokuda, T. Ohta, R. Matsushima-Nishiwaki, S. Takai, O. Kozawa, Phosphatidylinositol 3-kinase/Akt autoregulates PDGF-BB-stimulated interleukin-6 synthesis in osteoblasts, J. Cell. Biochem 99 (2006) 1564–1571.

[8] C.T. Brighton, R.M. Hunt, Early histological and ultrastructural changes in medullary fracture callus, Am. J. Bone Joint Surg. 73 (1981) 832–847.

[9] A.M. Parfitt, Osteonal and hemi-osteonal remodeling: the spatial and temporal framework for signal traffic in adult human bone, J. Cell. Biochem. 55 (1994) 273–286.

[10] A. Erlebacher, E.H. Filvaroff, S.E. Gitelman, R. Derynck, Toward a molecular understanding of skeletal development, Cell 80 (1995) 371–378.

[11] N. Ferrara, T. Davis-Smyth, The biology of vascular endothelial growth factor, Endocr. Rev. 18 (1997) 4–25.

[12] H.P. Gerber, T.H. Vu, A.M. Ryan, J. Kowalski, Z. Werb, N. Ferrara, VEGF couples hypertrophic cartilage remodeling, ossification and angiogenesis during endochondral bone formation, Nat. Med. 5 (1999) 623–628.

[13] D.L. Goad, J. Rubin, H. Wang, A.H. Tashijian Jr., C. Patterson, Enhanced expression of vascular endothelial growth factor in human SaOS-2 osteoblast-like cells and murine osteoblasts induced by insulin-like growth factor I, Endocrinology 137 (1996) 2262–2268.

[14] D.S. Wang, K. Yamazaki, K. Nohtomi, K. Shizume, K. Ohsumi, M. Shibuya, H. Demura, K. Sato, Increase of vascular endothelial growth factor mRNA expression by 1,25-dihydroxyvitamin D_3 in human osteoblast-like cells, J. Bone Miner. Res. 11 (1996) 472–479.

[15] J.M. Schalaeppi, S. Gutzwiller, G. Finlenzeller, B. Fournier, 1,25-dihydroxyvitamin D_3 induces the expression of vascular endothelial growth factor in osteoblastic cells, Endocr. Res. 23 (1997) 213–229.

[16] C. Widmann, S. Gibson, M.B. Jarpe, G.L. Johnson, Mitogen-activated protein kinase: conservation of a three-kinase module from yeast to human, Physiol. Rev. 79 (1999) 143–180.

[17] H. Tokuda, A. Harada, K. Hirade, H. Matsuno, H. Ito, K. Kato, Y. Oiso, O. Kozawa, Incadronate amplifies prostaglandin $F_{2\alpha}$-induced vascular endothelial growth factor in osteoblasts: enhancement of MAP kinase activity, J. Biol. Chem. 278 (2003) 18930–18937.

[18] E. Zelzer, B.R. Olsen, Multiple roles of vascular endothelial growth factor (VEGF) in skeletal development, growth, and repair, Curr. Top. Dev. Biol. 65 (2005) 169–187.

[19] H. Sudo, H. Kodama, Y. Amagai, S. Yamamoto, S. Kasai, In vitro differentiation and calcification in a new clonal osteogenic cell line derived from newborn mouse calvaria, J. Cell. Biol. 96 (1983) 191–198.

[20] O. Kozawa, H. Tokuda, M. Miwa, J. Kotoyori, Y. Oiso, Cross-talk regulation between cyclic AMP production and phosphoinositide hydrolysis induced by prostaglandin E_2 in osteoblast-like cells, Exp. Cell Res. 198 (1992) 130–134.

[21] U.K. Laemmli, Cleavage of structural proteins during the assembly of the head of bacteriophage T4, Nature 227 (1970) 680–685.

[22] C.J. Vlahos, W.F. Matter, K.Y. Hui, R.F. Brown, A specific inhibitor of phosphatidylinositol 3-kinase, 2-(4-morpholinyl)-8-phenyl-4H-1-benzopyran-4-one (LY294002), J. Biol. Chem. 269 (1994) 5721–5728.

[23] A. Arcaro, M.P. Wymann, Wortmannin is a potent phosphatidylinositol 3-kinase inhibitor: the role of phosphatidylinositol 3,4,5-trisphosphate in neutrophil responses, Biochem. J. 296 (1993) 297–301.

[24] D.R. Alessi, A. Cuenda, P. Cohen, D.T. Dudley, A.R. Saltiel, PD98059 is a specific inhibitor of the activation of mitogen-activated protein kinase in vitro and in vivo, J. Biol. Chem. 270 (1995) 27489–27494.

[25] Y. Hanai, H. Tokuda, H. Ohta, R. Matsushita-Nishiwaki, S. Takai, O. Kozawa, Phosphotidylinositol 3-kinase/Akt autoregulates PDGF-BB-stimulated interleukin-6 synthesis in osteoblasts, J. Cell. Biochem. 99 (2006) 1564–1571.

[26] E. Canalis, S. Rydziel, Platelet-derived growth factor and the skeleton, Principles of Bone Biology, second ed., 2002, pp. 817–824.

JOURNAL OF BONE AND MINERAL RESEARCH
Volume 22, Number 3, 2007
Published online on December 18, 2006; doi: 10.1359/JBMR.061209

Negative Regulation by p70 S6 Kinase of FGF-2–Stimulated VEGF Release Through Stress-Activated Protein Kinase/c-*Jun* N-Terminal Kinase in Osteoblasts

Shinji Takai,[1] Haruhiko Tokuda,[1,2] Yoshiteru Hanai,[1,2] Atsushi Harada,[3] Eisuke Yasuda,[1] Rie Matsushima-Nishiwaki,[1] Hisaaki Kato,[1,4] Shinji Ogura,[4] Toshiki Ohta,[5] and Osamu Kozawa[1]

ABSTRACT: To clarify the mechanism of VEGF release in osteoblasts, we studied whether p70 S6 kinase is involved in basic FGF-2–stimulated VEGF release in osteoblast-like MC3T3-E1 cells. In this study, we show that p70 S6 kinase activated by FGF-2 negatively regulates VEGF release through SAPK/JNK in osteoblasts.

Introduction: Vascular endothelial growth factor (VEGF) plays an important role in bone metabolism. We have previously reported that fibroblast growth factor-2 (FGF-2) stimulates the release of VEGF through p44/p42 mitogen-activated protein (MAP) kinase and stress-activated protein kinase/c-*Jun* N-terminal kinase (SAPK/JNK) in osteoblast-like MC3T3-E1 cells and that FGF-2–activated p38 MAP kinase negatively regulates VEGF release. However, the mechanism behind VEGF release in osteoblasts is not precisely known.
Materials and Methods: The levels of VEGF released from MC3T3-E1 cells were measured by enzyme immunoassay. The phosphorylation of each protein kinase was analyzed by Western blotting. To knock down p70 S6 kinase in MC3T3-E1 cells, the cells were transfected with siRNA to target p70 S6 kinase.
Results: FGF-2 time-dependently induced the phosphorylation of p70 S6 kinase. Rapamycin significantly enhanced the FGF-2–stimulated VEGF release and VEGF mRNA expression. The FGF-2–induced phosphorylation of p70 S6 kinase was suppressed by rapamycin. Rapamycin markedly enhanced the FGF-2–induced phosphorylation of SAPK/JNK without affecting the phosphorylation of p44/p42 MAP kinase or p38 MAP kinase. SP600125, a specific inhibitor of SAPK/JNK, suppressed the amplification by rapamycin of the FGF-2–stimulated VEGF release similar to the levels of FGF-2 with SP600125. Finally, downregulation of p70 S6 kinase by siRNA significantly enhanced the FGF-2–stimulated VEGF release and phosphorylation of SAPK/JNK.
Conclusions: These results strongly suggest that p70 S6 kinase limits FGF-2–stimulated VEGF release through self-regulation of SAPK/JNK, composing a negative feedback loop, in osteoblasts.
J Bone Miner Res 2007;22:337–346. Published online on December 18, 2006; doi: 10.1359/JBMR.061209

Key words: p70 S6 kinase, fibroblast growth factor-2, vascular endothelial growth factor, osteoblasts, mitogen-activated protein kinase

INTRODUCTION

It is well known that osteoblasts synthesize basic fibroblast growth factor (FGF)-2, and FGF-2 is embedded in bone matrix.[1,2] FGF-2 expression in osteoblasts is detected during fracture repair.[3] Bone metabolism is strictly regulated by osteoblasts and osteoclasts, which are responsible for bone formation and bone resorption, respectively.[4] Therefore, it is thought that FGF-2 plays a pivotal role in fracture healing, bone remodeling, and osteogenesis.[5] We have previously reported that FGF-2 autophosphorylates FGF receptors 1 and 2 among four structurally related high affinity receptors in osteoblast-like MC3T3-E1 cells.[6] In addition, we reported that FGF-2 stimulates induction of heat shock protein 27 in these cells.[7]

Bone remodeling carried out by osteoclasts and osteoblasts is accompanied by angiogenesis and capillary outgrowth.[8,9] During bone remodeling, capillary endothelial cells provide the microvasculature. It is well recognized that the activities of osteoblasts, osteoclasts, and capillary endothelial cells are closely coordinated and regulate bone metabolism.[10] These functional cells are considered to influence one another through humoral factors and by direct cell-to-cell contact. Vascular endothelial growth factor

The authors state that they have no conflicts of interest.

[1]Department of Pharmacology, Gifu University Graduate School of Medicine, Gifu, Japan; [2]Department of Clinical Laboratory, National Hospital for Geriatric Medicine, National Center for Geriatrics and Gerontology, Obu, Aichi, Japan; [3]Department of Functional Restoration, National Hospital for Geriatric Medicine, National Center for Geriatrics and Gerontology, Obu, Aichi, Japan; [4]Department of Emergency and Disaster Medicine, Gifu University Graduate School of Medicine, Gifu, Japan; [5]Department of Internal Medicine, National Hospital for Geriatric Medicine, National Center for Geriatrics and Gerontology, Obu, Aichi, Japan.

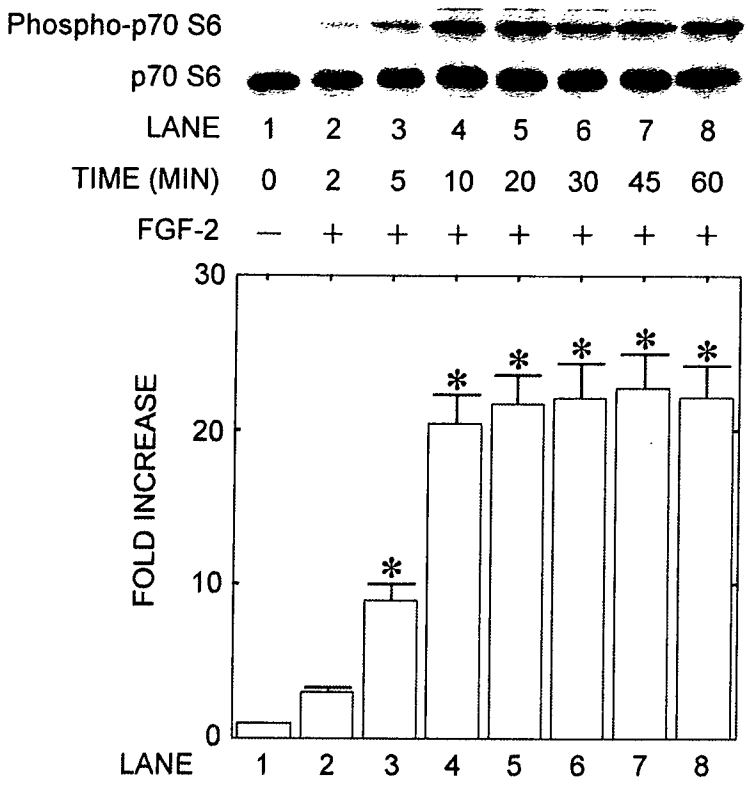

FIG. 1. Effect of FGF-2 on the phosphorylation of p70 S6 kinase in MC3T3-E1 cells. The cultured cells were stimulated by 70 ng/ml FGF-2 for the indicated periods. The extracts of cells were subjected to SDS-PAGE with subsequent Western blotting analysis with antibodies against phospho-specific p70 S6 kinase or p70 S6 kinase. The histogram shows quantitative representations of the levels of FGF-2–induced phosphorylation obtained from laser densitometric analysis of three independent experiments. Each value represents the mean ± SE of triplicate determinations. Similar results were obtained with two additional and different cell preparations. *$p < 0.05$ compared with the value of control.

(VEGF) is an angiogenic growth factor displaying high specificity for vascular endothelial cells.[11] VEGF, produced and secreted from a variety of cell types, increases capillary permeability and stimulates proliferation of endothelial cells.[11] As for bone metabolism, an inactivation of VEGF reportedly causes complete suppression of blood vessel invasion concomitant with impaired trabecular bone formation and expansion of hypertrophic chondrocyte zone in mouse tibial epiphyseal growth plate.[12] Evidence is accumulating that osteoblasts among bone cells produce and secrete VEGF in response to various physiological agents.[11,13–15] We have previously reported that FGF-2 stimulates VEGF release in MC3T3-E1 cells and that the release is positively regulated by p44/p42 mitogen-activated protein (MAP) kinase and stress-activated protein kinase/c-*Jun* *N*-terminal kinase (SAPK/JNK)[16,17] among the MAP kinase superfamily.[18] Based on these findings, it is currently recognized that VEGF secreted from osteoblasts may play an important role in the regulation of bone metabolism.[10,19] However, the mechanism behind VEGF synthesis in osteoblasts and its release from these cells is not fully understood.

p70 S6 kinase is a mitogen-activated serine/threonine kinase required for cell proliferation and G1 cell cycle progression.[20] As for osteoblasts, it has been shown that fluoroaluminate induces an increase in p70 S6 kinase phosphorylation.[21] In our previous study,[22] we reported that p70 S6 kinase plays as a positive regulator in bone morphogenetic protein-4–stimulated release of VEGF in osteoblast-like MC3T3-E1 cells. In addition, we recently showed that p38 MAP kinase, a member of the MAP kinase superfamily, functions at a point upstream from p70 S6 kinase in the release of VEGF in these cells.[23] However, the exact role of p70 S6 kinase in osteoblasts still remains unclear.

In this study, we investigated the involvement of p70 S6 kinase in the FGF-2–stimulated VEGF release in osteoblast-like MC3T3-E1 cells. We show that p70 S6 kinase activated by FGF-2 negatively regulates VEGF release through SAPK/JNK in these cells.

MATERIALS AND METHODS

Materials

FGF-2 and mouse VEGF enzyme immunoassay kits were purchased from R&D Systems (Minneapolis, MN, USA). Rapamycin and SP600125 were obtained from Calbiochem-Novabiochem Co. (La Jolla, CA, USA). Phospho-specific p70 S6 kinase antibodies, p70 S6 kinase antibodies, phospho-specific p44/p42 MAP kinase antibodies, p44/p42 MAP kinase antibodies, phospho-specific p38 MAP kinase antibodies, p38 MAP kinase antibodies, phospho-specific SAPK/JNK antibodies, and SAPK/JNK antibodies were purchased from Cell Signaling (Beverly, MA, USA). ECL Western blotting detection system was purchased from Amersham Biosciences (Piscataway, NJ, USA). Control short interfering RNA (siRNA; Silencer Negative Control no. 1 siRNA) or p70 S6 kinase siRNA (Silencer Predesigned siRNA, 75849, 75755, and 75942) was purchased from Ambion (Austin, TX, USA). siLentFect was pur-

chased from Bio-Rad (Hercules, CA, USA). Trizol reagent was purchased from Invitrogen (Carlsbad, CA, USA). Omniscript Reverse Transcriptase Kit was purchased from QIAGEN (Hilden, Germany). Fast-Start DNA Master SYBR Green I was purchased from Roche Diagnostics (Mannheim, Germany). Other materials and chemicals were obtained from commercial sources. Rapamycin or SP600125 was dissolved in dimethyl sulfoxide (DMSO). The maximum concentration of DMSO was 0.1%, which did not affect the assay for VEGF or Western blot analysis.

Cell culture

Cloned osteoblast-like MC3T3-E1 cells derived from newborn mouse calvaria[24] were maintained as previously described.[25] Briefly, the cells were cultured in α-MEM containing 10% FCS at 37°C in a humidified atmosphere of 5% CO_2/95% air. The cells were seeded into 35- (5×10^4) or 90-mm-diameter (5×10^5) dishes in α-MEM containing 10% FCS. After 5 days, the medium was exchanged for α-MEM containing 0.3% FCS. The cells were used for experiments after 48 h.

siRNA transfection

To knock down p70 S6 kinse in MC3T3-E1 cells, the cells were transfected with control siRNA (Silencer Negative Control no. 1 siRNA) or p70 S6 kinase siRNA (Silencer Predesigned siRNA, 75849, 75755, and 75942; Ambion) using the siLentFect (Bio-Rad) according to the manufacturer's protocol. In brief, the cells were seeded in a 35-mm-diameter (1×10^5) dish in α-MEM containing 10% FCS and subcultured for 48 h. After that, the cells were incubated at 37°C for 48 h with 250 nM siRNA-siLentFect complexes.

VEGF assay

The cultured cells were stimulated by various doses of FGF-2 in 1 ml of α-MEM containing 0.3% FCS for the indicated periods. When indicated, the cells were pretreated with rapamycin or SP600125 for 60 minutes. The conditioned medium was collected at the end of the incubation, and the VEGF concentration was measured by ELISA kit.

Western blot analysis

The cultured cells were stimulated by FGF-2 in α-MEM containing 0.3% FCS for the indicated periods. The cells were washed twice with PBS, lysed, homogenized, and sonicated in a lysis buffer containing 62.5 mM Tris/HCl, pH 6.8, 2% SDS, 50 mM dithiothreitol, and 10% glycerol. The cytosolic fraction was collected as a supernatant after centrifugation at 125,000*g* for 10 minutes at 4°C. SDS-PAGE was performed according to Laemmli[26] in 10% polyacrylamide gel. Western blotting analysis was performed as described previously[27] using phospho-specific p70 S6 kinase antibodies, p70 S6 kinase antibodies, phospho-specific p44/p42 MAP kinase antibodies, p44/p42 MAP kinase antibodies, phospho-specific p38 MAP kinase antibodies, p38 MAP kinase antibodies, phospho-specific SAPK/JNK antibodies, or SAPK/JNK antibodies, with peroxidase-labeled antibodies raised in goat against rabbit IgG being used as second

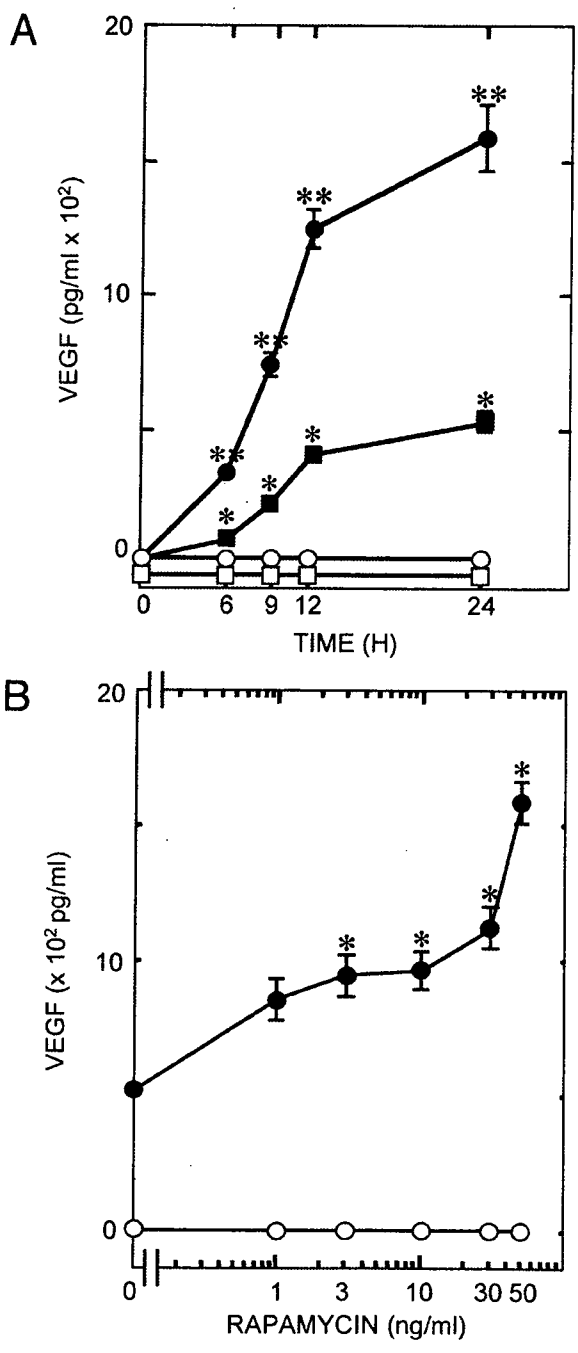

FIG. 2. Effect of rapamycin on the FGF-2–stimulated VEGF release in MC3T3-E1 cells. (A) The cultured cells were pretreated with 10 ng/ml rapamycin (circle symbols) or vehicle (square symbols) for 60 minutes and stimulated by 70 ng/ml FGF-2 (solid symbols) or vehicle (open symbols) for the indicated periods. $*p < 0.05$ compared with the control. $**p < 0.05$ compared with the value of FGF-2 alone. (B) The cultured cells were pretreated with various doses of rapamycin for 60 minutes and stimulated by 70 ng/ml FGF-2 (●) or vehicle (○) for 24 h. $*p < 0.05$ compared with the value of FGF-2 alone. Each value represents the mean ± SE of triplicate determinations. Similar results were obtained with two additional and different cell preparations.

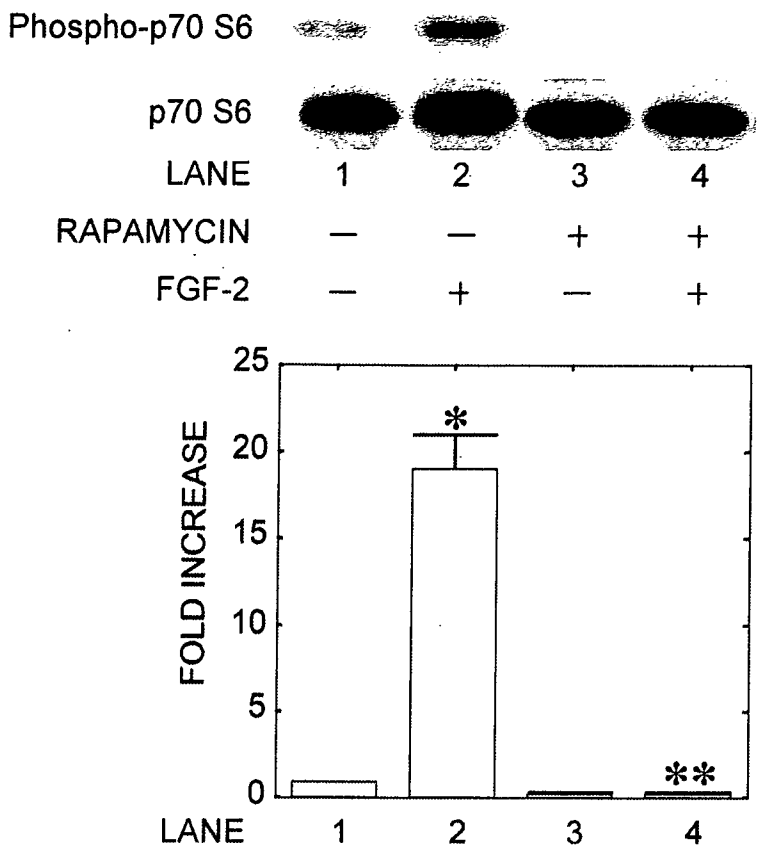

FIG. 3. Effect of rapamycin on the FGF-2–induced phosphorylation of p70 S6 kinase in MC3T3-E1 cells. The cultured cells were pretreated with 10 ng/ml rapamycin or vehicle for 60 minutes and stimulated by 30 ng/ml FGF-2 or vehicle for 10 minutes. The extracts of cells were subjected to SDS-PAGE with subsequent Western blotting analysis with antibodies against phospho-specific p70 S6 kinase or p70 S6 kinase. The histogram shows quantitative representations of the levels of FGF-2–induced phosphorylation obtained from laser densitometric analysis of three independent experiments. Each value represents the mean ± SE of triplicate determinations. Similar results were obtained with two additional and different cell preparations. *$p < 0.05$ compared with the control. **$p < 0.05$ compared with the value of FGF-2 alone.

antibodies. Peroxidase activity on the polyvinylidene difluoride (PVDF) sheet was visualized on X-ray film by means of the electrochemiluminescence (ECL) Western blotting detection system.

Determination

The absorbance of enzyme immunoassay samples was measured at 450 nm with EL 340 Bio Kinetic Reader (Bio-Tek Instruments, Winooski, VT, USA). The densitometric analysis was performed using Molecular Analyst/Macintosh (Bio-Rad Laboratories).

Real-time RT-PCR

The cultured cells were pretreated with rapamycin and/or SP600125 and stimulated by FGF-2 for the indicated time period. Total RNA was isolated and transcribed into cDNA using Trizol reagent and Omniscript Reverse Transcriptase Kit. Real-time PCR was performed using a Light Cycler system (Roche Diagnostics) in capillaries and Fast-Start DNA Master SYBR Green I provided with the kit. Sense and antisense primers were synthesized based on the report of Simpson et al.[28] for mouse VEGF mRNA and GAPDH mRNA. The amplified products were determined by melting curve analysis and agarose electrophoresis. VEGF mRNA levels were normalized with those of GAPDH mRNA.

Statistical analysis

The data were analyzed by ANOVA followed by the Bonferroni method for multiple comparisons between pairs, and $p < 0.05$ was considered significant. All data are presented as the mean ± SE of triplicate determinations. Each experiment was repeated three times with similar results.

RESULTS

Effect of FGF-2 on the phosphorylation of p70 S6 kinase in MC3T3-E1 cells

To study whether FGF-2 activates p70 S6 kinase in osteoblast-like MC3T3-E1 cells, we examined the effect of FGF-2 on the phosphorylation of p70 S6 kinase. The stimulation of FGF-2 time-dependently induced the phosphorylation of p70 S6 kinase (Fig. 1). The maximum effect was observed at 20 minutes after the stimulation of FGF-2.

Effect of rapamycin on the FGF-2–stimulated VEGF release in MC3T3-E1 cells

To clarify whether p70 S6 kinase is involved in the FGF-2–induced release of VEGF in MC3T3-E1 cells, we examined the effect of rapamycin, a specific inhibitor of p70 S6